The Meteoritical Society

Meteoritics & Planetary Science 48, Nr 11, 2155–2165 (2013)
doi: 10.1111/maps.12160

Challenges in detecting olivine on the surface of 4 Vesta

Andrew W. BECK[1*], Timothy J. McCOY[1], Jessica M. SUNSHINE[2], Christina E. VIVIANO[3], Catherine M. CORRIGAN[1], Takahiro HIROI[4], and Rhiannon G. MAYNE[5]

[1]Department of Mineral Sciences, Smithsonian Institution, Washington, District of Columbia 20560–0112, USA
[2]Department of Astronomy, University of Maryland, College Park, Maryland 20742–2421, USA
[3]Johns Hopkins University Applied Physics Laboratory, Laurel, Maryland 20723, USA
[4]Department of Geological Sciences, Brown University, Providence, Rhode Island 02912, USA
[5]Department of Geology, Texas Christian University, Fort Worth, Texas 76129, USA
[*]Corresponding author. E-mail: becka@si.edu

(Received 25 November 2012; revision accepted 14 June 2013)

Abstract–Identifying and mapping olivine on asteroid 4 Vesta are important components to understanding differentiation on that body, which is one of the objectives of the Dawn mission. Harzburgitic diogenites are the main olivine-bearing lithology in the howardite-eucrite-diogenite (HED) meteorites, a group of samples thought to originate from Vesta. Here, we examine all the Antarctic harzburgites and estimate that, on scales resolvable by Dawn, olivine abundances in putative harzburgite exposures on the surface of Vesta are likely at best in the 10–30% range, but probably lower due to impact mixing. We examine the visible/near-infrared spectra of two harzburgitic diogenites representative of the 10–30% olivine range and demonstrate that they are spectrally indistinguishable from orthopyroxenitic diogenites, the dominant diogenitic lithology in the HED group. This suggests that the visible/near-infrared spectrometer onboard Dawn (VIR) will be unable to resolve harzburgites from orthopyroxenites on the surface of Vesta, which may explain the current lack of identification of harzburgitic diogenite on Vesta.

INTRODUCTION

One of the primary goals of the Dawn mission at 4 Vesta is to test hypotheses that have been proposed for the geologic evolution of that asteroid (Russell and Raymond 2011). These hypotheses are largely based on petrologic studies of howardite, eucrite, and diogenite (HED) meteorites, a group of mafic achondrites originating from Vesta (McSween et al. 2013). The diogenites, which come from the lower crust/upper mantle of Vesta, are primarily two different lithologies. The majority of the samples are orthopyroxenites composed almost entirely of orthopyroxene, and there are a few of the more recently recognized harzburgites, containing mixtures of orthopyroxene and olivine (Beck and McSween 2010). The harzburgites have also been called "olivine diogenites" (e.g., Sack et al. 1991), a term which will not be used here. One brecciated dunitic diogenite, composed almost entirely of olivine, was also recently identified (A. Beck et al. 2011). It is widely accepted that the diogenites formed through fractional crystallization (versus partial melting), although the geologic setting for that fractionation is still unclear.

Magma ocean-style fractionation has traditionally been preferred for the origin of the diogenites, and is supported by a perceived uniformity in diogenite pyroxene major element concentrations across many of the samples (Ikeda and Takeda 1985; Ruzicka et al. 1997; Warren 1997). Fractionation from a magma ocean would result in a layered sequence from an Mg-rich dunitic mantle, to upper mantle/lower crustal harzburgites, followed by an orthopyroxenite layer. Magma ocean fractionation would probably lead to these lithologies forming at relatively uniform depths across Vesta. Other studies have proposed that diogenite fractionation occurred in multiple plutons, not a single magmatic system. Variation in trace element concentrations (Mittlefehldt 1994; Fowler et al. 1995; Barrat et al. 2008) and overlap in pyroxene major

elements between harzburgitic and orthopyroxenitic diogenite lithologies (Beck and McSween 2010; Shearer et al. 2010) support a serial magmatism model. Similarly, the petrology and geochemistry of the one dunitic diogenite suggest that it may be crustal cumulate as well (A. Beck et al. 2011), although the paucity of this lithology in the HED suite dictates caution when incorporating dunite into diogenite petrogenetic models. In a serial magmatism scenario, multiple diogenite plutons would be emplaced at varied depths within the crust and fractionate to produce layered sequences of harzburgite overlain by orthopyroxenite, with the possibility of basal dunitic cumulates in some cases. On a global scale, serial magmatism would lead to a nonuniform distribution and depth of these lithologies on Vesta. Note that the magma ocean and serial magmatism models are not mutually incompatible for the formation of dunites, harzburgites, and orthopyroxenites (i.e., the Moon); thus, it is also possible that a hybrid model is appropriate for the diogenites.

Different petrogenetic models proposed for the diogenites can be tested by mapping the distribution of harzburgite and orthopyroxenite, the most prominent diogenite lithologies based on meteorite data, where they are exposed on the surface of Vesta. Observations have revealed several large impact basins, which presumably sample to depths that expose these diogenite lithologies (Thomas et al. 1997; Jaumann et al. 2012). Mapping the distribution of harzburgite and orthopyroxenite might be possible using reflectance data returned by NASA's Dawn spacecraft, which recently finished orbital mapping of asteroid 4 Vesta. If the diogenite lithologies are found consistently at an approximately equal depth, this would support magma ocean-style fractionation as the dominant method for diogenite petrogenesis. Conversely, if diogenitic lithologies occur at varied depths, diogenite formation in multiple plutons would be favored.

Prior to trying to map the distributions of diogenitic lithologies, however, it is important to establish whether the harzburgite lithology is resolvable from the more dominant orthopyroxenite lithology, given the spectral and spatial resolution of the instruments on board Dawn. VIR, a visible/near-infrared (VNIR, 0.3–2.5 μm) spectrometer on Dawn, is the primary instrument used to map the surface mineralogy of Vesta (De Sanctis et al. 2011). VIR collects hyperspectral data over two channels with spectral ranges of 0.25–1.05 μm (VIS) and 1.0–5.0 μm (IR), at spectral resolutions of 1.8 and 9.8 nm band^{-1}, respectively. At Dawn's low altitude mapping orbit (LAMO) VIR has an optimal spatial resolution of approximately 70 m pixel^{-1} (De Sanctis et al. 2012a), although the practical spatial resolution required to resolve lithologic variation is probably somewhat higher.

To test if the orthopyroxenitic and harzburgitic diogenite lithologies are spectrally distinct, the spectral characteristics of the minerals that make up each lithology must be characterized. Orthopyroxene (opx) exhibits two well-defined absorption features at approximately 1 and 2 μm (BI and BII, respectively), the former being the stronger of the two. In contrast, olivine (ol) has a broader, asymmetric BI feature, relative to opx, centered at approximately 1.2 μm and has no BII absorption feature. These absorption features result from electronic transitions in Fe^{2+} cations in the mineral structure and shift toward longer wavelengths with increasing Fe^{2+} content, and increasing Ca^{2+} content in pyroxene (e.g., Adams 1974). Because of the spectral differences in opx and ol, rocks composed of opx + ol (harzburgites) should be distinguishable from pure opx samples (orthopyroxenites) via a broadening of the BI feature, a shift in BI center to longer wavelengths, and a reduced BII feature with increasing olivine abundance (Singer 1981). Thus, BI center may be used to constrain olivine abundances in mixtures of opx + ol, as it shifts to longer wavelengths with the addition of olivine. However, BI may also shift to longer wavelengths due to increasing Fe^{2+} and/or Ca^{2+} content in opx (Adams 1974), and disorder of Fe^{2+} and Mg^{2+} in the pyroxene M1 and M2 sites can lead to decreased spectral contrast (difference in reflectance intensities between continuum and absorption) of the BI and BII features as well (Besancon et al. 1991). Minimizing variability in opx compositions and mineral structure between samples where BI features are being observed mitigates the probability of erroneously attributing a shift in BI from mineralogic differences (e.g., different opx composition) to varying proportions of olivine and opx. In this study, we constrain mineralogic differences between samples, so that shifts in BI can be more accurately attributed to olivine abundance. In studies involving remote sensing techniques (i.e., VIR data from Vesta), other methods should be used to constrain opx chemistry (i.e., BII position) prior to examining variation in olivine abundance between orthopyroxenitic and harzburgitic lithologies to avoid the pitfalls discussed above.

The broadening of the BI feature and reduction of the BII feature can be quantitatively represented by a band area ratio (BAR), or BII area/BI area (Cloutis et al. 1986). To calculate BAR, first two linear continuums are fit to the BI and BII absorption features. The BI continuum is a linear fit between the wavelength of maximum reflectance near 0.7 μm and the inflection between the BI and BII absorption at

approximately 1.4–1.7 μm. Typically, the BII continuum is a linear fit between the same wavelength of maximum reflectance at the inflection (approximately 1.4–1.7 μm) and 2.5 μm (as the longward wing of the BII absorption is incomplete) (e.g., Cloutis et al. 1986). However, some authors choose to anchor the BII continuum fit to wavelengths <2.5 μm (e.g., 2.3 μm) due to laboratory settings where atmospheric water can modify the BII absorption feature (e.g., P. Beck et al. 2011). Differences in conventions for fitting the BII continuum do not allow BAR values to be directly compared between techniques (e.g., Vernazza et al. 2008). For example, selecting an anchor for the BII continuum at shorter wavelengths leads to lower BAR values (higher inferred olivine abundances) relative to those calculated for the same spectrum using an anchor point at a longer wavelength for the BII fit. Therefore, comparisons can only be made between samples where BAR values are calculated using the same BII continuum fit endpoints (i.e., BAR values using a 2.3 μm anchor point cannot be compared to the mixing models of Cloutis et al. 1986).

The areas of BI and BII are calculated by resolving the area between the continuum and the spectrum, as bound by the ranges reported above. These areas are ratioed to achieve the BAR calculation for an individual spectrum. An increase in BAR value is inferred as an increase in the proportion of opx to olivine. The advantage of using the BAR versus the BI center calculation is that BAR is relatively unaffected by grain size variation, as long as both phases have similar particle size distributions, and that a linear relationship exists between % opx/(opx + ol) and BAR, resolvable to ±5–10% abundances (e.g., Cloutis et al. 1986).

Olivine distribution in harzburgitic diogenites is very heterogeneous (e.g., Bowman et al. 1997) and the olivine abundance expected for a hypothetical ~70 m (one LAMO VIR pixel) exposure of pure harzburgite on Vesta is not well constrained. The petrologic portion of this study aims to constrain the olivine abundance expected for harzburgite exposures on the surface of Vesta by measuring olivine abundances from multiple thin sections of each of the Antarctic harzburgites. Although the total number of Antarctic harzburgites is small (four meteorites, approximately 1.7 kg total mass), by utilizing all samples, we present the best estimate of olivine abundance given the data that are available. Results from the petrologic portion of this study were then used to select a subset of harzburgite samples for spectral analysis that have olivine abundances most representative of a putative large-scale harzburgitic lithology. We then test the resolvability of the harzburgitic diogenites from the more common orthopyroxenitic diogenites by comparing laboratory VNIR spectra of the selected samples from the two lithologic groups. If the two lithologies are not resolvable in a laboratory setting, it is unlikely that Dawn will be able to accurately map their distribution on the surface of Vesta, leaving one of the main questions about vestan petrogenetic history unanswered.

METHODS

We examine 3-6 thin sections and splits from all of the harzburgitic diogenites recovered in Antarctica, which include: Asuka (A) 881548, Allan Hills (ALH) 77256, Graves Nunataks (GRA) 98108, and Miller Range (MIL) 07001. The individual thin section and split numbers used in this study are listed in Table 1. While members of the LaPaz Icefield (LAP) 03979 pairing group have been described as unbrecciated harzburgites (McCoy and Welzenbach 2004), other studies propose that they may be olivine-rich polymict breccias (Beck and McSween 2010), and they will not be considered here. We exclude harzburgitic diogenites recovered in Northwest Africa (NWA), primarily because they are from hot desert environments, which can lead to alteration materials having a significant effect on the VNIR spectra (e.g., calcite and iron oxide). We also restrict our study to Antarctic meteorites due to the well-characterized nature of those collections, a crucial component to the petrologic portion of this work. All petrographic observations and analyses were conducted using a FEI Nova Nano Scanning Electron Microscope 600 (SEM) and a JEOL 8900 Superprobe Electron Microprobe (EMP) at the Smithsonian National Museum of Natural History. SEM imaging was conducted using a ≤5 nA electron beam under both high- and low-vacuum modes (high vac = thin sections, low vac = sample splits). EMP thin section analyses were conducted using a 15 kV, 20 nA electron beam with a 2 μm spot size. Elemental count times on the EMP ranged from 20 to 30 s. Thin section modal abundances were calculated from backscatter electron (BSE) images using the image processing software Environment for Visualizing Images (ENVI 4.8, ITT Visual Information Solutions, Boulder, Colorado, USA), similar to methods described in Beck et al. (2012b).

Approximately 500 mg sample splits of harzburgites GRA 98108 and MIL 07001 were requested for spectral analysis. The reason for choosing these two harzburgites is explained in the Petrology and Spectra sections. The splits were first coarsely crushed into a few pieces and examined on the SEM to confirm olivine abundances that were observed in thin section. The coarsely crushed splits were then ground to <45 μm powders and

Table 1. Olivine abundances and grain sizes in the Antarctic harzburgitic diogenites.

Sample	Section no.	Normalized mode			Average OL grain size (mm)	Reference
		PLAG	OPX	OL		
A-881548	31-1	n.d.	54	46	10	Yamaguchi et al. (2011)
	51-2	n.d.	20	80	10	Yamaguchi et al. (2011)
	23 (split)	n.d.	100[a]	0[a]	–	Barrat et al. (2008)
	Average (±1s)		58	42 (40)	10	
ALH 77256	99	n.d.	64	36	1.35	Sack et al. (1991)
	116	n.d.	100	0	–	Bowman et al. (1997)
	115	n.d.	99	1	–	Bowman et al. (1997)
	128	<1	89	11	1.90	Beck and McSween (2010)
	5	n.d.	97	3	0.95	This study
	Average		90	10 (15)	1.40 (0.5)	
GRA 98108	16	<1	81	19	0.35	Beck and McSween (2010)
	2	<1	68	32	0.30	This study
	15	<1	70[a]	30[a]	0.45	Righter (2001)
	Average		73	27 (7)	0.36 (0.1)	
MIL 07001	2	n.d.	91	9	0.15	This study
	6	n.d.	87[b]	13[b]	0.10	This study
	16 (slab)	n.d.	90[a]	10[a]	–	This study
	40	n.d.	87	13	0.10	This study
	55	n.d.	91	9	0.15	This study
	54	n.d.	90	10	0.20	This study
	Average		89	11 (2)	0.14 (0.1)	
	Group average		77	23 (15)		

PLAG = plagioclase; OPX = orthopyroxene; OL = olivine; n.d. = either not determined, or measured and <0.1 vol%; <1 = value between 0.1 and 0.9 vol%.

[a]Estimated modes, all others calculated from BSE images.

[b]13 vol% olivine is a more accurate abundance for this section than that reported in Tkalcec and Brenker (2012) (Tkalcec, personal communication).

analyzed using the UV-VIS-NIR bidirectional spectrometer at Brown University's KECK/NASA Reflectance Experiment Laboratory (RELAB). All measurements were made at 30° incidence and 0° emission angles, and spectra were sampled at 5 nm intervals in the 0.28–2.6 μm spectral range. We compare the harzburgite spectra to those of the orthopyroxenitic diogenite Tatahouine, which were acquired by Michael J. Gaffey at RELAB under similar conditions to those described above for the harzburgitic diogenites. As this study focuses on spectral variations between the orthopyroxenitic and harzburgitic diogenite lithologies that can be linked to olivine abundance, care was taken to assure that olivine abundance was the only VNIR spectra-altering feature that differed between the samples from each lithology. The constraining of other variables that could affect VNIR absorption features is explained in the Spectra section.

The linear continuum removal procedure described in the Introduction for determination of BI and BII was applied to the harzburgitic and orthopyroxenitic diogenite spectra. Then, BARs, BI, and BII centers were all calculated using the continuum-removed spectra. BI and BII centers are typically calculated using an nth-order polynomial fit to the continuum-removed region around the BI and BII absorption features, respectively, where n is a value between 3 and 8, determined by the fit that minimizes the linear least square residual (e.g., Gaffey et al. 1993). The regions surrounding the BI and BII absorption minimums were set at ±10 channels (or 100 nm) for the determination of the band centers via polynomial fitting.

We calculate BAR values using the methods described in the Introduction after Cloutis et al. (1986), and thus a comparison of BAR values between this study and Cloutis et al. (1986) is justified. We calculated uncertainties in our BAR calculations by propagating 1σ variations from the original reflectance data, which are a combination of system noise and variation in reflectance as the sample is spun. The individual errors in reflectance at each wavelength were combined through standard propagation of error with the calculation of each band area. As band areas are approximated by finding the area between the spectrum and a line, the propagation of errors for each area was relatively straightforward (linear combinations),

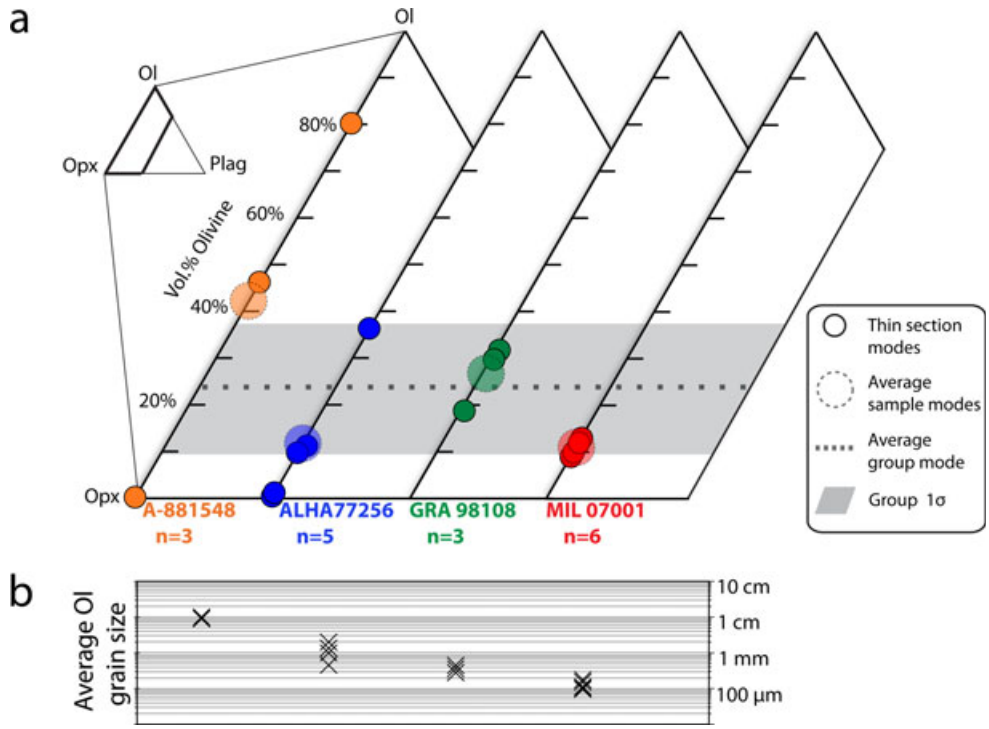

Fig. 1. a) Olivine (Ol), orthopyroxene (Opx), plagioclase (Plag) abundances for multiple thin sections (small colored circles) from the four Antarctic harzburgitic diogenites (color coded, one per quadrilateral). Samples are listed in order of decreasing intrasample variation in olivine abundance from left to right. Average sample olivine abundances (larger, translucent circles) and average olivine abundance across the entire group (gray dashed line, ±1σ gray area) are also shown. b) Average olivine grain size in the thin sections is plotted under each associated sample quadrilateral, where decreasing average grain size (left to right) correlates with decreasing intrasample variation in olivine abundance shown above.

resulting in BAR uncertainties of ±0.01. P. Beck et al. (2011) conducted a more complete calculation of uncertainties associated with laboratory-derived BAR values in HEDs. In that study, P. Beck et al. (2011) collected 17 spectra from a single eucrite, each spectrum collected with different measurement angles. They then calculated the variance in 17 BAR values derived from each of the eucrite spectra, resulting in a BAR uncertainty of ±0.05. We will use the P. Beck et al. (2011) BAR uncertainties for the duration of this work.

In an effort to compare our diogenite results to a more robust set of BAR values from mixtures with known opx + ol abundances, we also calculate BARs from spectra of opx/ol mixtures created by Corrigan et al. (2007) and McCoy et al. (2007). The mixtures analyzed in those studies consist of San Carlos olivine and opx from the Johnstown diogenite in proportions ranging from 10% ol: 90% opx to 90% ol: 10% opx in 20% steps (i.e., 90% ol, 70% ol, etc.). Spectra of pure San Carlos olivine and Johnstown opx were also collected. The spectra of these mixtures were obtained at RELAB using the bidirectional spectrometer, and measured at similar conditions to those used for the orthopyroxenitic and harzburgitic diogenite splits (<45 µm grain size, 5 nm data interval, $e = 30°$, $i = 0°$). BARs of the San Carlos ol/Johnstown opx mixtures were calculated with the same method used for the orthopyroxenite and harzburgite diogenite splits. As it is a diogenite, Johnstown opx compositions are comparable to those from other samples in the group, while San Carlos olivine (Fo_{90}, Jarosewich et al. 1980) has a higher Mg# than diogenitic olivine (max diogenite ol Fo = 78, Shearer et al. 2010).

RESULTS

Petrology

The Antarctic harzburgites have a range of intrasample (between thin sections from one sample) variations in olivine abundance. Olivine/opx abundances for multiple thin sections of each sample appear in Table 1 and are plotted in Fig. 1a, where they are listed in order of decreasing intrasample variation from top to bottom (Table 1) and left to right (Fig. 1a). Large intrasample olivine abundance variation was observed in A-881548 and ALH 77256, while harzburgitic diogenites GRA 98108 and MIL 07001 are relatively

more uniform in olivine distribution. Variation in olivine abundance within the samples appears to be correlated with mean olivine grain size (Table 1; Fig. 1b). Samples with average olivine grain sizes in the order of millimeters to a centimeter (A-881548 and ALH 77256) have much larger intrasample variation in olivine abundance than samples with grain sizes in the approximately 100–400 μm range (GRA 98108 and MIL 07001). The large variation in olivine abundance for samples with millimeter- to centimeter-sized grains is probably due to the fact that thin section size (the sampling size) is on the order of centimeters as well.

Average olivine abundances for entire samples were calculated by averaging all the thin section abundances together. Weighted averages were not used; all thin sections modes within a sample were valued equally. Average sample olivine abundances range from 11% (MIL 07001) to 42% (A-881548). These sample averages were used to calculate average olivine abundance for the entire group, which is 23% with a 15% 1σ deviation from the mean (Table 1; Fig. 1a). Weighted averages were not used to compute the group average either. The large 1σ (relative to the mean) is primarily due to the limited number of samples ($n = 4$) combined with a single outlier, A-881548 (42% olivine). If A-881584 is omitted, the sample averages fall within a tighter approximately 10–30% range in olivine abundance, which may be a better estimate for olivine abundance for a putative large harzburgite exposure on Vesta. The total number of samples examined here is too small to statistically rule out A-881548 as an outlier. However, the tighter 10–30% olivine range hypothesized for putative harzburgite exposures on the surface of Vesta can be tested by examining the abundance of olivine in brecciated harzburgites. In theory, a brecciated harzburgite should be a homogenized sampling of a relatively large harzburgite exposure on the surface of Vesta. Beck and McSween (2010) note that dimict diogenite breccias (a breccia mixture of harzburgitic + orthopyroxenitic diogenite clasts) Lewis Cliff (LEW) 88679 and Meteorite Hills (MET) 01084 contain 14.6 and 6.1 vol% olivine, respectively. Here, we calculate the olivine abundances in only the harzburgitic portions of those two dimict breccias using fig. 3 of Beck and McSween (2010), where brecciated areas that are clearly harzburgite are denoted. Note that we threshold image values to exclude all phases in the orthopyroxenitic portion of the breccias from our calculations and only measure the abundance of olivine relative to other phases in the harzburgitic portions of those breccias. We calculate olivine abundances of 26 vol% in the harzburgitic portion of LEW 88679,8 and 12 vol% in the harzburgitic portion of MET 01084,5. These calculations support the approximately 10–30 vol% range in olivine abundance predicted previously, not the broader approximately 10–45 vol% range when A-881548 is included.

Spectra

Given the results from the petrologic portion of this study, harzburgitic diogenites GRA 98108 (GRA) and MIL 07001 (MIL) appear to be the best candidates for spectral characterization: They have olivine abundances within the 10–30% range hypothesized for putative harzburgite exposures on the surface of Vesta and have limited intrasample olivine abundance variation. Limited intrasample variation in olivine abundance increases the chance that the splits used for spectral analysis will have olivine abundances like those observed in thin section. Orthopyroxenes in GRA and MIL are very similar in composition, approximately Wo_2 En_{76} and Wo_1 En_{76}, respectively. Olivine is also similar in both samples (approximately Fo_{72}). GRA and MIL also contain negligible (<1%) amounts of high-Ca pyroxene. Like olivine, the presence of high-Ca pyroxene (HCP) and increased Fe concentration in opx can shift BI and BII absorption features in the VNIR (Adams 1974). If opx Fe concentrations and the presence of HCP are not constrained between the harzburgitic and orthopyroxenitic diogenites examined here, we cannot conclusively identify differences in spectra solely attributable to olivine abundance. We select the orthopyroxenitic diogenite Tatahouine for spectral comparison to the harzburgites because: (1) it has very similar opx compositions to the harzburgites examined here (Tatahouine = Wo_2 En_{75}, Mittlefehldt 1994; harzburgites GRA and MIL = approximately Wo_2 En_{76}), (2) it is well characterized as lacking olivine and HCP (Bowman et al. 1997), and (3) as an observed fall it should be relatively free of alteration materials. Likewise, the powders of Tatahouine used for spectral analysis are similar in size to those of the two harzburgitic diogenites (Tatahouine = <25 μm, harzburgites GRA and MIL = <45 μm). Also, given the protracted cooling time of both the orthopyroxenitic and harzburgitic diogenite lithologies, it seems unlikely that there would be variation in the ordering in pyroxene structures between harzburgite and orthopyroxenite to sufficiently change the reflectivity of BI and BII absorption features between samples.

As mentioned previously, the splits of GRA and MIL were examined on the SEM prior to grinding for spectral analysis to confirm the petrology observed in thin section. In the split of MIL, relatively small, equigranular olivine grains were observed in roughly the same abundance as observed in thin section (Fig. 2). Likewise, the split of GRA had a similar petrology to the thin sections observed in this study.

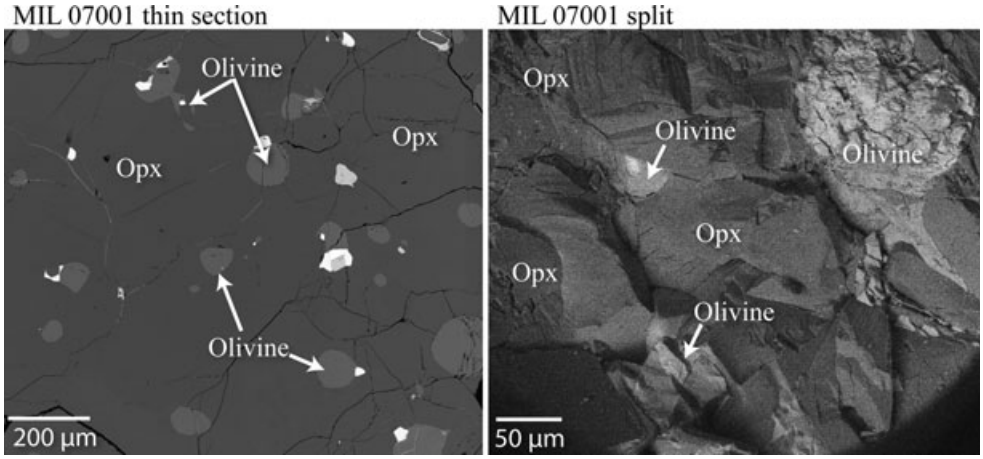

Fig. 2. BSE images from the MIL 07001,2 thin section (left) and the MIL 07001 coarsely ground sample split prior to powdering for spectral analysis (right). The thin section and split show similar phase abundances and textures. Note the images were taken at different magnification levels and at different analytic conditions; the latter leading to phases having different grayscale thresholds between images.

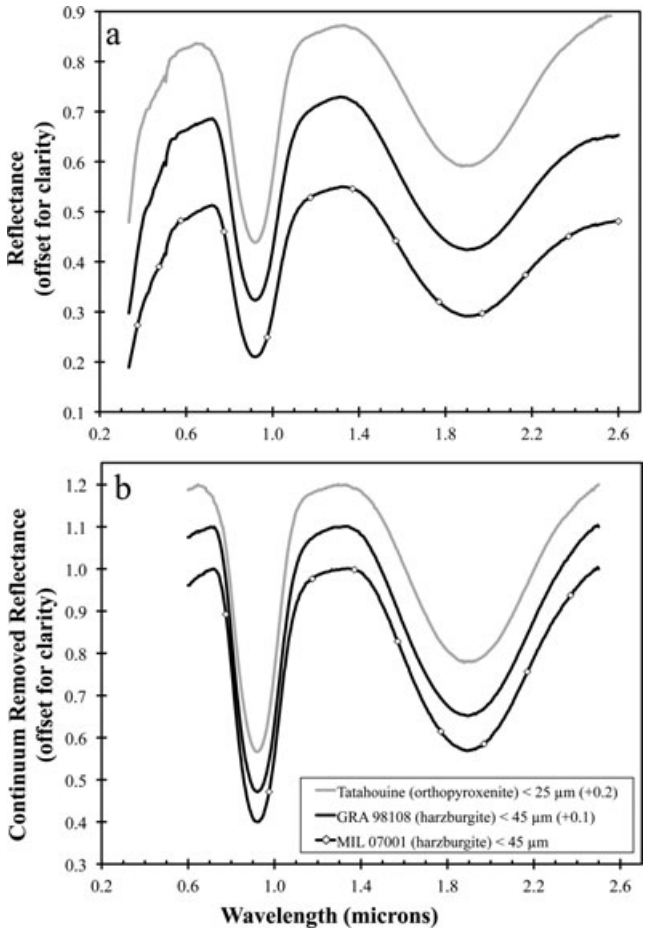

Fig. 3. a) VNIR reflectance spectra of harzburgitic diogenites (ol + opx) MIL 07001 and GRA 98108 compared to the spectra of orthopyroxenitic diogenite (opx) Tatahouine. b) Reflectance spectra of all three samples with the continuum removed via a linear fitting procedure described in the Introduction. Spectra have been offset for clarity by intervals of 0.1.

BI and BII absorption features between the harzburgites and the orthopyroxenite are nearly indistinguishable (Fig. 3). In the continuum-removed spectra, the BI centers calculated for both harzburgitic diogenites (MIL and GRA = 0.92 μm) are identical to the wavelength calculated for the orthopyroxenitic diogenite BI center (Tatahouine = 0.92 μm). Similarly, the BII centers calculated for the harzburgitic diogenites (MIL = 1.89 and GRA = 1.89 μm) are very near and almost indistinguishable to the orthopyroxenitic diogenite BII center (Tatahouine = 1.88 μm). There does not appear to be any reduction in the BII feature of the harzburgitic diogenites, which is quantitatively expressed by BAR. The harzburgitic diogenites have BARs of 1.89 ± 0.05 and 1.88 ± 0.05 (GRA and MIL, respectively), and, again, are very similar to the orthopyroxenitic diogenite Tatahouine, which has a BAR of 1.74 ± 0.05. Given analytic uncertainty, the BAR values of the harzburgitic and orthopyroxenitic diogenites vary only by approximately 0.04. Because BAR values can vary within the orthopyroxenitic diogenite lithology alone by approximately 0.3 (P. Beck et al. 2011), a 0.04 difference between the two lithologies is likely insignificant.

The BARs of the ol/opx mixtures calculated for this study follow the trend previously established by Cloutis et al. (1986); BARs decrease with increased olivine abundance in the mixtures. However, a discernible decrease in BAR is not observed in the Cloutis et al. (1986) data until olivine concentrations are ≥30%, with BAR values for mixtures with 0–25% overlapping within a 1σ variance (Beck et al. 2012a). Thus, the data by Cloutis et al. (1986) support the conclusion that diogenites with 10–25% olivine (harzburgites) will be difficult to discern from 100% opx diogenites (orthopyroxenites) using BAR (Fig. 4).

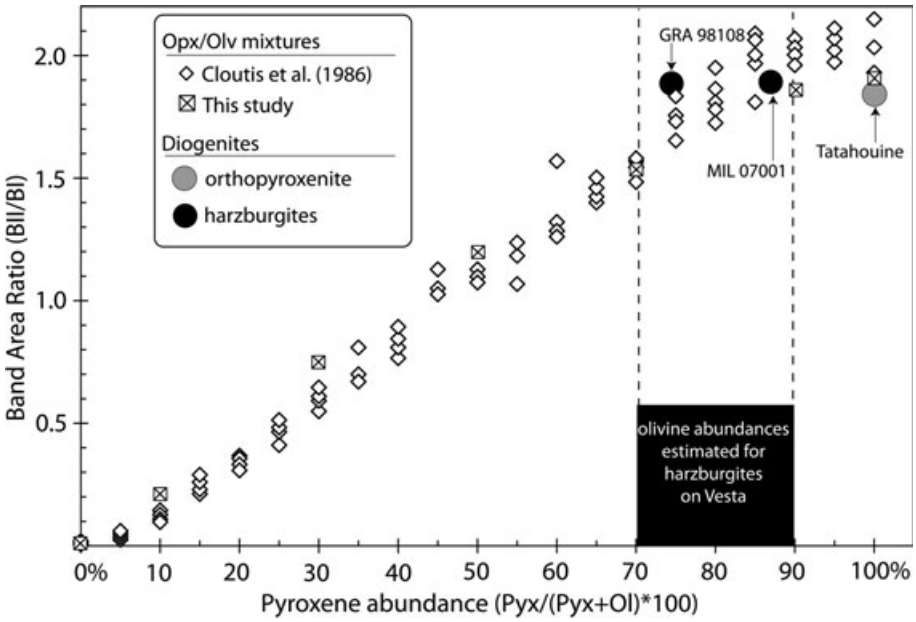

Fig. 4. Band area ratio for orthopyroxene (Pyx)/olivine (Ol) mixtures from this study and Cloutis et al. (1986), along with those from two harzburgitic and one orthopyroxenitic diogenite measured here. The estimated range of olivine abundances for large exposures of harzburgite on Vesta is also shown. Olivine abundances in harzburgitic diogenites are too low to resolve them from orthopyroxenitic diogenites using BAR, suggesting that it will be difficult to distinguish harzburgites and orthopyroxenites on Vesta with VIR data.

DISCUSSION

The lack of significant shift in absorption features to longer wavelengths, lack of a reduction in the BII feature, and lack of decreased BAR in the harzburgites relative to the orthopyroxenite would seem to suggest that the harzburgite splits measured here do not contain any olivine. This cannot be the case because the splits were examined with an SEM prior to powdering, and olivine abundances representative of those observed in thin section were confirmed (Fig. 2). An alternative hypothesis is that olivine abundances in harzburgitic diogenites MIL and GRA are too low to effectively alter their spectra, making them spectrally indistinguishable from the orthopyroxenitic diogenite Tatahouine. The hypothesis that the olivine abundance is too low to alter the BI and BII features can be tested by examining changes in absorption features from opx mixtures with the addition of various amounts of olivine. As previously discussed, Cloutis et al. (1986) conducted an experiment examining the effect on BAR of Wo_0 En_{86} opx mixtures with the addition of various amounts of Fo_{89} olivine. Note that the olivine and opx grains used in those mixtures are more Mg-rich than those in the diogenites examined here (mixtures = olivine Mg# 89 and opx Mg# 86 [Singer 1981; Cloutis et al. 1986] versus diogenites = olivine Mg# 73 and opx Mg# 77 [this study]). Cloutis et al. (1986) calculated the BAR of several sets of mixtures with the same opx/ol abundance, but varied grain sizes ranging from 63 to 125 μm. We combine these data with the BAR calculations of our opx/ol mixtures and present them in Fig. 4, where the BARs of the diogenite samples are also shown. The BAR data from opx/ol mixtures compiled here demonstrate that samples with 10–25% olivine are very difficult to distinguish from 100% opx samples using BAR. Significantly lower BARs appear in samples with ≥30% olivine; however, these are greater olivine abundances than hypothesized for large-scale vestan harzburgite exposures based on our analysis of meteorites in the collection. The BAR mixture data are consistent with the findings of this study, where harzburgitic diogenites with 11 and 27% olivine have nearly identical BARs to an orthopyroxenitic diogenite with approximately 100% opx.

Cloutis et al. (1986) also examined another BAR (henceforth BAR*) defined as BII area*/BI area*, where BII area* is the area on the shorter side the BII minimum that is enclosed by the spectral curve, a tangent line from the 1.4–1.7 μm infliction point, and a line perpendicular to the BII minimum. BI area* is BI area multiplied by a ratio of the 0.4/0.7 μm reflectance. The primary reason for BAR* is to mitigate spectral interfaces from OH, which can have absorption features in the longer wavelength regions of the BII feature. In their study Cloutis et al. (1986) report BAR* values ranging from 0.82 to 1.11 for 100% opx. GRA and

MIL, the harzburgitic diogenites from this study, both have BAR* values of 1.10, suggesting that BAR* cannot be used to distinguish orthopyroxenite from harzburgite on the surface of Vesta either.

It is important to note that a large exposure of pure dunitic diogenite on Vesta, which would contain ≥90% olivine (A. Beck et al. 2011), would presumably be distinguishable using BAR from surrounding opx-dominated rocks. A study by P. Beck et al. (2011) examined the spectral properties of diogenite NWA 4223. A report in the Meteoritical Bulletin identifies NWA 4223 as an "olivine diogenite" (aka harzburgitic diogenite) and reports one section containing approximately 50% olivine and very coarse olivine grains, up to 4 mm (Connolly et al. 2007). P. Beck et al. (2011) report a BAR of approximately 1.2 for NWA 4223, distinguishing this sample from all orthopyroxenitic diogenites in that study, which had BARs of approximately 1.5–2.5. No petrologic information about NWA 4223 is reported in the spectral study by P. Beck et al. (2011); however, given the identification of millimeter-sized grains by Connolly et al. (2007), it is presumable that the approximately 1 g split used for spectral analysis (P. Beck et al. 2011) contained a few, large olivine grains. As discussed in the Petrology section, and plotted in Fig. 1, harzburgitic diogenites with very large olivine grains (like A-881548 and ALH 77256) are the most heterogeneous samples of the group, and small splits from those samples are likely not representative of harzburgite exposures on the surface of Vesta that are on scales resolvable by VIR. Thus, the spectra reported for the 1 g split of NWA 4223 is probably not applicable to distinguishing harzburgite from orthopyroxenite on the surface of Vesta. However, it does demonstrate that opx/ol mixtures with diogenitic compositions do follow BAR trends anticipated for higher concentrations of olivine. Therefore, if diogenitic lithologies that contain very high concentrations of olivine (i.e., dunite) are exposed over large scales on the surface of Vesta, they should be discernible using BAR.

In the Petrology section, we hypothesize that a putative harzburgite exposure on the surface of Vesta that is on the scale of one VIR LAMO pixel will have olivine abundances in the 10–30% range. Given this estimate, and given the spectral results presented earlier in this section, it is likely that VIR will have difficulty distinguishing harzburgite from orthopyroxenite on the surface of Vesta. Therefore, one interpretation for the current lack of identification of harzburgite exposures on surface Vesta by Dawn (DeSanctis et al. 2012b) is that they are present, but spectrally irresolvable from surrounding orthopyroxenitic diogenite. It is important to note that the 10–30% range predicted here would be for "pristine" harzburgite exposures. As Vesta is one of the oldest stable surfaces in the solar system, and as diogenites are hypothesized to come from the lower crust, it is unlikely that diogenitic lithologies, which formed approximately 4.5 Ga (Takahashi and Masudat 1990), remain as "pristine" intact surface exposures, at least on VIR-pixel scales. Thus, the 30% upper limit of olivine abundance we hypothesize for approximately 60 m exposures of harzburgite is a best-case scenario. A realistic upper limit is somewhat lower due to impact mixing and dilution of olivine abundance. Perhaps the range of olivine abundances observed in bulk dimict diogenite breccias, like the 6–16% range observed in the breccias MET 01084 and LEW 88679 (Beck and McSween 2010), is more appropriate. Therefore, the lack of olivine detection on the surface of Vesta is probably due in most part to the relatively low initial abundance of olivine in the primary rocks, but also resultant from olivine dilution through impact gardening.

CONCLUSIONS

1. Grain size and sample homogeneity are important factors to consider when selecting meteorite samples for representative spectral analyses of planetary surfaces.
2. Here, we demonstrate that harzburgitic diogenite meteorites (opx + ol) are heterogeneous in olivine abundance, and we hypothesize that pristine exposures of harzburgite on the surface of Vesta will contain 10–30% olivine on spatial scales resolvable by the Dawn spacecraft.
3. Laboratory VNIR spectral results show that representative harzburgitic samples are not spectrally distinct from the more dominant, orthopyroxenitic diogenite lithology (pure opx). Analysis of BARs of ol/opx mixtures strongly suggests that the lack of resolvability of the harzburgites is due to their relatively low olivine abundances.
4. This study provides an explanation for the current lack of definitive harzburgite detection on the surface of Vesta by the Dawn spacecraft. While the lack of detection is primarily attributable to the relatively low olivine abundances in the harzburgites, the protracted impact history of the surface of 4 Vesta was probably also a factor, diluting olivine concentrations through impact gardening.

Acknowledgments—We thank D. W. Mittlefehldt, B. J. Tkalcec, and K. Righter for providing images and information about harzburgitic diogenite thin sections; the Antarctic Search for Meteorites Program for recovering the samples studied here; and V. Reddy for

opx/olivine mixture compositional data. This manuscript was improved by comments from the AE, D. W. Mittlefehldt, and reviews by E. Cloutis and an anonymous reviewer. Funding was provided by a NASA Dawn at Vesta Participating Scientist Grant to T. J. McCoy.

Editorial Handling—Dr. David Mittlefehldt

REFERENCES

Adams J. B. 1974. Visible and near-infrared diffuse reflectance spectra of pyroxenes as applied to remote sensing of solid objects in the solar system. *Journal of Geophysical Research* 79:4829.

Barrat J. A., Yamaguchi A., Greenwood R. C., Benoit M., Cotten J., Bohn M., and Franchi I. A. 2008. Geochemistry of diogenites; still more diversity in their parental melts. *Meteoritics & Planetary Science* 43:1759–1775.

Beck A. W. and McSween H. Y. 2010. Diogenites as polymict breccias composed of harzburgite and orthopyroxenite. *Meteoritics & Planetary Science* 45:850–872.

Beck A. W., Mittlefehldt D., McSween H., Rumble D., Lee C.-T., and Bodnar R. 2011. MIL 03443, a Dunite from asteroid 4 Vesta: Evidence for its classification and cumulate origin. *Meteoritics & Planetary Science* 46:1133–1151.

Beck P., Barrat J. A., Grisolle F., Quirico E., Schmitt B., Moynier F., Gillet P., and Beck C. 2011. NIR spectral trends of HED meteorites: Can we discriminate between the magmatic evolution, mechanical mixing and observation geometry effects? *Icarus* 216:560–571.

Beck A. W., Sunshine J. M., McCoy T. J., and Hiroi T. 2012a. Challenges to finding olivine on the surface of 4 Vesta (abstract #2218). 43rd Lunar and Planetary Science Conference. CD-ROM.

Beck A. W., Welten K. C., McSween H. Y., Viviano C. E., and Caffee M. W. 2012b. Petrologic diversity among the PCA 02 howardite group, one of the largest pieces of the vestan surface. *Meteoritics & Planetary Science* 47:947–969.

Besancon J. R., Burns R. G., and Pratt S. F. 1991. Reflectance spectra of Fe^{2+}-Mg^{2+} disordered pyroxenes: Implications to remote-sensed spectra of planetary surfaces. 12th Lunar and Planetary Science Conference. p. 1048.

Bowman L. E., Spilde M. N., and Papike J. J. 1997. Automated energy dispersive spectrometer modal analysis applied to the diogenites. *Meteoritics & Planetary Science* 32:869–875.

Cloutis E. A., Gaffey M. J., Jackowski T. L., and Reed K. L. 1986. Calibrations of phase abundances, composition and particle size distribution for olivine-orthopyroxene mixtures from reflectance spectra. *Journal of Geophysical Research* 91:11641–11653.

Connolly H. C., Jr., Smith C., Benedix G., Folco L., Righter K., Zipfel J., Yamaguchi A., and Chennaoui Aoudjehane H. 2007. The Meteoritical Bulletin, No. 92. *Meteoritics & Planetary Science* 42:1647–1694.

Corrigan C. M., McCoy T. J., Sunshine J. M., Bus S. J., and Gale A. 2007. Does spectroscopy provide evidence for widespread partial melting of asteroids? I. Mafic mineral abundances (abstract #1463). 38th Lunar and Planetary Science Conference. CD-ROM.

De Sanctis M. C., Coradini A., Ammannito E., Fliacchione G., Capria M. T., Fonte S., Magni G., Barbis A., Bini A., Dami M., Ficai-Veltroni I., and Preti G. 2011. The VIR spectrometer. *Space Science Reviews* 163:329–369.

De Sanctis M. C., Ammannito E., Capaccioni F., Capria M. T., Carraro F., Fonte S., Frigeri A., Longobardo A., Magni G., Marchi S., Palomba E., Tosi F., Zambon F., Combe J. P., McCord T. B., McFadden L. A., McSween H. Y., Mittlefehldt D. W., Pieters C. M., Raymond C. A., Russell C. T., Jaumann R., Stephan K., and Sunshine J. 2012a. Dawn at Vesta: Distribution of different minerals (abstract). European Planetary Science Conference #446.

DeSanctis M. C., Ammannito E., Capria M. T., Tosi F., Capaccioni F., Zambon F., Carraro F., Fonte S., Frigeri A., Jaumann R., Magni G., Marchi S., McCord T. B., McFadden L. A., McSween H. Y., Mittlefehldt D. W., Nathues A., Palomba E., Pieters C. M., Raymond C. A., Russell C. T., Toplis M. J., and Turrini D. 2012b. Spectroscopic characterization of mineralogy and its diversity across Vesta. *Science* 336:697–700.

Fowler G. W., Shearer C. K., and Papike J. J. 1995. Diogenites as asteroidal cumulates: Insights from orthopyroxene trace element chemistry. *Geochimica et Cosmochimica Acta* 59:3071–3084.

Gaffey M. J., Bell J. F., Brown R. H., Burbine T. H., Piatek J. L., Reed K. L., and Chaky D. A. 1993. Mineralogical variations within the S-type asteroid class. *Icarus* 106:573–602.

Ikeda Y. and Takeda H. 1985. A model for the origin of basaltic achondrites based on the Yamato 7308 howardite. Proceedings of the 15th Lunar and Planetary Science Conference. *Journal of Geophysical Research* 90:C649–C663.

Jarosewich E., Nelen J. A., and Norberg J. A. 1980. Reference samples for electron microprobe analysis. *Geostandards Newsletter* 4:43–47.

Jaumann R., Williams D. A., Buczkowski D. L., Yingst R. A., Preusker F., Hiesinger H., Schmedemann N., Kneissl T., Vincent J. B., Blewett D. T., Buratti B. J., Carsenty U., Denevi B. W., De Sanctis M. C., Garry W. B., Keller H. U., Kernten E., Krohn K., Li J.-Y., Marchi S., Matz K. D., McCord T. B., McSween H. Y., Mest S. C., Mittlefehldt D. W., Mottola S., Nathues A., Neukum G., O'Brien D. P., Pieters C. M., Prettyman T. H., Raymond C. A., Roatsch T., Russell C. T., Schenk P., Schmidt B. E., Scholten F., Stephan L., Sykes M. V., Tricarico P., Wagner R., Zuber M. T., and Sierks H. 2012. Vesta's shape and morphology. *Science* 336:687–694.

McCoy T. J. and Welzenbach L. 2004. Thin section (,2) description. *Antarctic Meteorite Newsletter* 27:19.

McCoy T. J., Corrigan C. M., Sunshine J. M., Bus S. J., and Gale A. 2007. Does spectroscopy provide evidence for widespread partial melting of asteroids? II. Pyroxene compositions (abstract #1631). 38th Lunar and Planetary Science Conference. CD-ROM.

McSween H. Y., Binzel R. P., De Sanctis M. C., Ammannito E., Prettyman T. H., Beck A. W., Reddy V., Le Corre L., Gaffey M. J., Raymond C. A., Russell C. T., and the Dawn Science Team. 2013. Dawn, the Vesta-HED connection, and the geologic context for eucrites, diogenites, and howardites. *Meteoritics & Planetary Science* 48, doi:10.1111/maps.12108.

Mittlefehldt D. W. 1994. The genesis of diogenites and HED parent body petrogenesis. *Geochimica et Cosmochimica Acta* 58:1537–1552.

Righter K. 2001. Petrography, mineralogy and petrology of two new HED meteorites; diogenite GRA 98108 and howardite GRA 98030 (abstract #1765). 32nd Lunar and Planetary Science Conference. CD-ROM.

Russell C. T. and Raymond C. A. 2011. The Dawn mission to Vesta and Ceres. *Space Science Reviews* 163:3–23.

Ruzicka A., Snyder G. A., and Lawrence L. A. 1997. Vesta as the howardite, eucrite and diogenite parent body: Implications for the size of a core and for large-scale differentiation. *Meteoritics & Planetary Science* 32:825–840.

Sack R. O., Azeredo W. J., and Lipschutz M. E. 1991. Olivine diogenites: The mantle of the eucrite parent body. *Geochimica et Cosmochimica Acta* 55:1111–1120.

Shearer C. K., Burger P., and Papike J. J. 2010. Petrogenetic relationships between diogenites and olivine diogenites: Implications for magmatism on the HED parent body. *Geochimica et Cosmochimica Acta* 74:4865–4880.

Singer R. B. 1981. Near-infrared spectral reflectance of mineral mixtures: Systematic combinations of pyroxenes, olivine, and iron oxides. *Journal of Geophysical Research* 86:7967–7982.

Takahashi K. and Masudat A. 1990. Young ages of two diogenites and their genetic implications. *Nature* 343:540–542.

Thomas P. C., Binzel R. P., Gaffey M. J., Storrs A. D., Wells E. N., and Zellner B. H. 1997. Impact excavation of asteroid 4 Vesta: Hubble Space Telescope results. *Science* 227:1492–1495.

Tkalcec B. J. and Brenker F. E. 2012. Plastic deformation of olivine-rich diogenites and implications for mantle processes on asteroid 4 Vesta (abstract #5327). 75th Meteoritical Society Meeting.

Vernazza P., Binzel R. P., Thomas C. A., DeMeo F. E., Bus S. J., Rivkin A. S., and Tokunaga A. T. 2008. Compositional differences between meteorites and near-Earth asteroids. *Nature* 454:858–860.

Warren P. H. 1997. Magnesium oxide-iron oxide mass balance constraints and a more detailed model for the relationship between eucrites and diogenites. *Meteoritics & Planetary Science* 32:945–963.

Yamaguchi A., Barrat J.-A., Ito M., and Bohn M. 2011. Posteucritic magmatism on Vesta: Evidence for the petrology and thermal history of diogenites. *Journal of Geophysical Research* 116:E08009.